

Regional Influence of Aerosol Emissions from Wildfires Driven by Combustion Efficiency: Insights from the BBOP Campaign

Sonya Collier,[†] Shan Zhou,[†] Timothy B. Onasch,[‡] Daniel A. Jaffe,^{§,¶} Lawrence Kleinman,^{||} Arthur J. Sedlacek, III,^{||} Nicole L. Briggs,^{§,¶,⊥} Jonathan Hee,[§] Edward Fortner,[‡] John E. Shilling,[#] Douglas Worsnop,[‡] Robert J. Yokelson,[∇] Caroline Parworth,[†] Xinlei Ge,[†] Jianzhong Xu,[†] Zachary Butterfield,[○] Duli Chand,[#] Manvendra K. Dubey,[○] Mikhail S. Pekour,[#] Stephen Springston,^{||} and Qi Zhang^{*,†}

[†]Department of Environmental Toxicology, University of California, Davis, California 95616, United States

[‡]Aerodyne Research Inc., Billerica, Massachusetts 01821, United States

[§]School of Science and Technology, University of Washington, Bothell, Washington 98011, United States

[¶]Department of Atmospheric Sciences, University of Washington, Seattle, Washington 98195, United States

^{||}Environmental and Climate Sciences Department, Brookhaven National Laboratory, Upton, New York 11973, United States

[⊥]Gradient, Seattle Washington 98101, United States

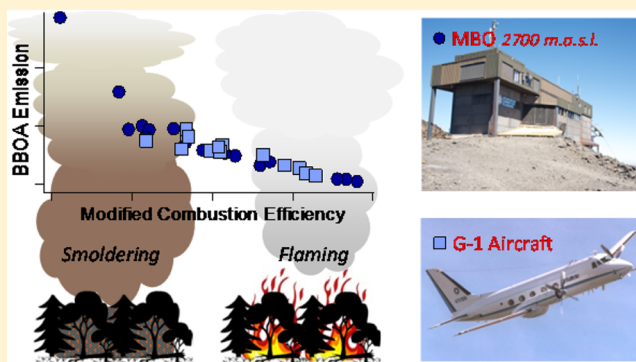
[#]Atmospheric Sciences and Global Change Division, Pacific Northwest National Laboratory, Richland, Washington 99352, United States

[∇]Department of Chemistry, University of Montana, Missoula, Montana 59812, United States

[○]Earth and Environmental Sciences Division, Los Alamos National Laboratory, Los Alamos, New Mexico 87545, United States

Supporting Information

ABSTRACT: Wildfires are important contributors to atmospheric aerosols and a large source of emissions that impact regional air quality and global climate. In this study, the regional and nearfield influences of wildfire emissions on ambient aerosol concentration and chemical properties in the Pacific Northwest region of the United States were studied using real-time measurements from a fixed ground site located in Central Oregon at the Mt. Bachelor Observatory (~2700 m a.s.l.) as well as near their sources using an aircraft. The regional characteristics of biomass burning aerosols were found to depend strongly on the modified combustion efficiency (MCE), an index of the combustion processes of a fire. Organic aerosol emissions had negative correlations with MCE, whereas the oxidation state of organic aerosol increased with MCE and plume aging. The relationships between the aerosol properties and MCE were consistent between fresh emissions (~1 h old) and emissions sampled after atmospheric transport (6–45 h), suggesting that biomass burning organic aerosol concentration and chemical properties were strongly influenced by combustion processes at the source and conserved to a significant extent during regional transport. These results suggest that MCE can be a useful metric for describing aerosol properties of wildfire emissions and their impacts on regional air quality and global climate.



INTRODUCTION

Biomass burning (BB) is one of the largest sources of trace gases and carbonaceous aerosols on a global scale and has intense adverse effects on air quality and human health.^{1–4} Emissions from wildfires and other BB sources, such as agricultural and residential wood burning, also influence Earth's climate via a combination of direct,^{2,5} indirect^{6,7} and semidirect effects.^{8,9} Wildfires, in particular, are a large and highly variable component of BB emissions¹⁰ and typically an “uncontrollable” source of aerosols that can cause haze in pristine areas and poor

air quality at downwind sites.^{11,12} Many factors, such as fuel type, burn conditions, and atmospheric aging, can influence the chemical and microphysical properties of BB aerosols. The organic component, namely biomass burning organic aerosol (BBOA), is a dominant component in BB fine aerosols^{13,14} and

Received: April 1, 2016

Revised: June 23, 2016

Accepted: July 11, 2016

Published: July 11, 2016

thus influences their hygroscopicity and optical properties, which are important parameters for assessing the impacts of BB emissions on regional air quality and global climate. However, BBOA are compositionally complex and their characteristics and impacts are poorly represented in models.

An important property of a BB event which strongly affects emission characteristics is the modified combustion efficiency (MCE) – an index of the relative amount of smoldering and flaming. The MCE is defined as the unitless molar ratio of the enhanced concentration of CO₂ over the background to the sum of the enhanced concentrations of CO and CO₂: $MCE = \Delta CO_2 / (\Delta CO + \Delta CO_2)$.^{15,16} Higher MCE (>0.9) is associated with most of the emissions being processed by flaming combustion, whereas lower MCE (<0.9) is associated with mostly smoldering combustion, where pyrolysis and gasification emissions escape flame processing.^{16,17} Various studies have demonstrated that emission factors for particulate matter (PM) and trace gases in BB are strongly influenced by MCE^{18–21} and that lower MCE is usually associated with increased PM emissions per unit of fuel burned.^{22–24}

So far, much of the information on BB emissions comes from prescribed and agricultural fires and very little is known about the characteristics of BBOA and their correlation with MCE for wildfires, especially in the midlatitude region. In order to fill this knowledge gap, we examine plumes from wildfires in the Pacific Northwest region of the United States using data acquired in summer 2013 during the Department of Energy (DOE) sponsored Biomass Burning Observation Project (BBOP). The BBOP campaign combined aircraft and ground measurement platforms to study both gas and particle phase emissions using real-time instruments and collected one of the most extensive data sets on wildfires performed in the contiguous U.S. Here, we report the chemical characteristics of nonrefractory submicrometer aerosols (NR-PM₁) measured by two high-resolution time-of-flight aerosol mass spectrometers (HR-AMS) in regional and near-field wildfire plumes with a range of transport times (1 h to 2 days) and their relationships to MCE and atmospheric aging that potentially refine representation of BB emissions in models for more accurate assessments of wildfire impacts.

EXPERIMENTAL METHODS

2.1. Campaign Description and Instrument Deployment.

As shown in Figure 1, various instances of strong and persistent wildfire activity in the Pacific Northwest region were reported by satellite data during the campaign period (July 25th to August 25th, 2013) and many wildfire plumes were sampled at a fixed site located at Mt. Bachelor Observatory (MBO; 43.979 °N, 121.687 °W, ~ 2700 m a.s.l.). In addition, fresher (~1 h aging) plumes from the Whiskey Fire Complex and more aged plumes (4–10 h) transported from the Salmon River Fire Complex were sampled extensively by the Gulfstream G-1 aircraft on Aug. sixth and 16th, respectively (Figure 1).

A comprehensive suite of real-time instruments, including HR-AMS^{25,26} and measurements of aerosol optical properties and gas-phase tracer concentrations, were deployed on board the G-1 aircraft and at MBO during BBOP. The HR-AMS provides detailed chemical information on the nonrefractory (NR) portion of PM₁ at fast time-resolution and its high-resolution mass spectra help identify various sources for observed ambient aerosol and determine the average elemental ratios of organic components.^{26–28} At MBO, the HR-AMS was

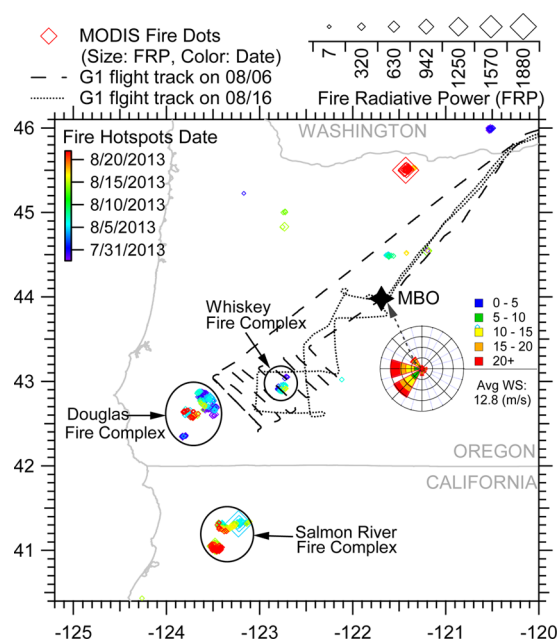


Figure 1. Map of the Pacific Northwest U.S. with the location of MBO and two G-1 aircraft flight trajectories shown. Open diamonds represent fires detected by the MODIS satellite during the period spanning the measurement campaign and are colored by date and sized by fire radiative power (FRP). Persistent and large-scale wildfires are highlighted by circles. The inset polar graph represents the statistical distribution of wind direction and speed at MBO during July 25 to August 25, 2013.

operated in the ion optical “V-mode” and sampled alternatively, every 5 min, downstream of a thermodenuder instrument and through an ambient bypass line (see Figure S1 and section 1.1.1 in the Supporting Information (SI)). For the purposes of this analysis, only bypass information is discussed.

The G-1 platform measured aerosol composition using an HR-AMS equipped with an intracavity laser, which is called the Soot-Particle Aerosol Mass Spectrometer (SP-AMS²⁹). Aerosol particles were sampled from outside of the G-1 using a forward facing two-stage diffuser aerosol inlet system.³⁰ Inside the G-1, PM₁ were sampled into the SP-AMS through a 130 μm diameter critical orifice from a constant pressure inlet operating at a pressure of ~620 Torr.³¹ The SP-AMS alternated between “laser-on” mode, for the measurement of refractory black carbon and associated coatings, and “laser-off” mode, which functions identically to a standard HR-AMS. In this study we focus on data acquired in “laser-off” mode, that is, as a standard HR-AMS, in “V-mode”. However, unlike the HR-AMS at MBO, the SP-AMS on the G-1 was operated in “Fast-MS” mode with 1 s sampling time.^{32,33}

Additional descriptions of measurements and instrumentation during BBOP are given in the SI. Table S1 contains quality control and assurance information such as limit of detections, ionization efficiencies, and relative ionization efficiencies for both MBO and G-1. Influences from gas-phase CO₂ on the particulate organic CO₂⁺ signal were subtracted in a time-dependent manner using gas-phase CO₂ data³⁴ for both platforms. All the data reported here has been converted to standard temperature and pressure (STP, 273 K, 1 atm) conditions.

2.2. Back Trajectory Analysis and Estimation of Plume Transport Times.

The locations and times of active fires in

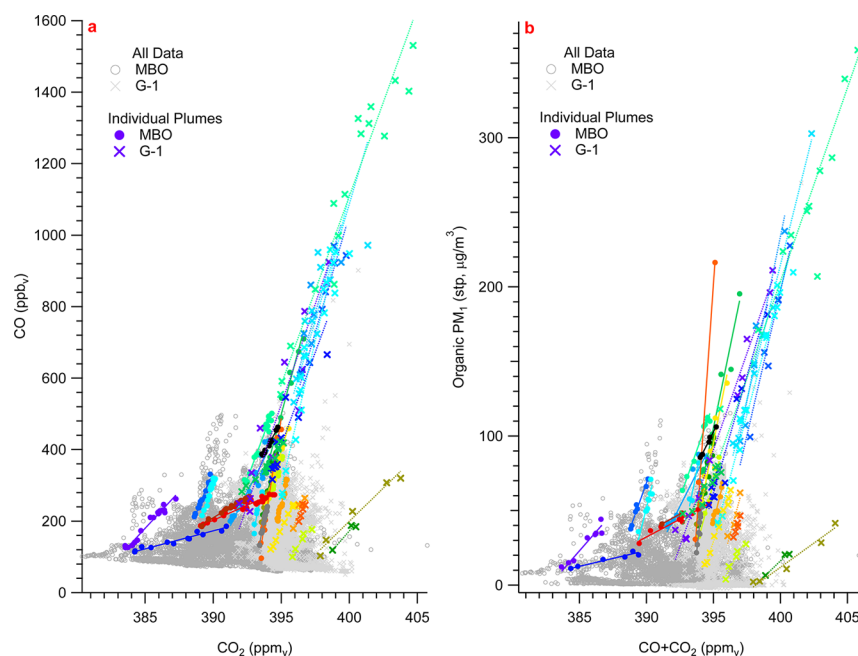


Figure 2. Scatter plots of (a) gas-phase CO vs CO₂ in ppbv/ppmv, and (b) particulate organics vs CO+CO₂ in µgm⁻³/ppmv. Plumes measured at MBO and by the G-1 aircraft, and selected for enhancement ratio calculation, are shown as individually colored markers. Pearson's r^2 , slope, and intercepts are summarized in SI Table S2.

the region, detectable by the MODIS instrument aboard the Aqua and Terra satellites, were downloaded from the NASA operated Fire Information Resource Management System (<https://firms.modaps.eosdis.nasa.gov>, near real-time collection 5 type data was used). In order to identify possible plume sources, 3-day back trajectory analysis was performed using the HYSPLIT model (Hybrid Single Particle Lagrangian Integrated Trajectory archive data, available at <http://ready.arl.noaa.gov/HYSPLIT.php>).³⁵ HYSPLIT results were compared with MODIS fire hotspot information (SI Figure S3–S17), where overlap of trajectories with hotspots both verified wildfire emission source locations and provided estimated plume transport times. In cases where multiple sources were possible candidates or where source or transport time was ambiguous, forward trajectory analysis was performed using 40 km resolution meteorological data (EDAS). Average and ranges for transport time for each plume were estimated based on a combination of both forward and back trajectory results. When plumes were sampled by G-1 the flight path coordinates were used as starting points for back trajectory analysis. When the G-1 location coincided very closely to a MODIS fire hotspot, it was assumed that plumes were approximately 1 h old, in order to allow for plume rise. Air mass relative humidity (RH) values along calculated trajectories were also derived via HYSPLIT back trajectory analysis.

RESULTS AND DISCUSSION

3.1. Identification of Wildfire Plumes and Calculation of MCE and Enhancement Ratios. Near combustion sources, emission factors and emission ratios are commonly calculated for use in emissions inventories.⁴ However, MCE and enhancement ratios (ERs) can be calculated for emissions sampled downwind of a fire source by taking the ratio of the enhancement of a species of interest above background to the enhancement of a stable representative plume tracer. ERs may also be calculated by finding the linear regression slope between

a parameter of interest and the plume tracer when multiple, well-correlated measurements are available at a specific distance downwind.^{36,37} Changing backgrounds, particularly when plumes enter a different air mass such as the free troposphere, can impact calculation of MCE and ERs for trace gases and particulate species in BB plumes.³⁸ However, uncertainty for ER calculations is much reduced when emissions of parameters of interest are significantly higher than their background values.^{37,38}

In this study, we identify wildfire plumes and determine MCEs and ERs for selected periods when concentrations of CO, CO₂, organic PM, and major organic ions in the HR-AMS spectra are all well above their corresponding background levels and the correlations among these parameters are high for selected plumes.³⁹ The high correlation criterion is chosen to minimize background and mixing effects on MCE and ER calculations. In this study, a total of 32 plumes, 18 from MBO and 14 from G-1, are identified and the correlations between CO and CO₂ and between organic PM and ΣC (= CO+CO₂) are high for each plume ($r^2 > 0.85$; Figure 2 and SI Table S2). Due to the stringent criteria, plumes in this analysis make up a small percentage of all campaign data (e.g., 1.3% of MBO data). The correlations between HR-AMS organic ions and ΣC are high for all the plumes as well (e.g., SI Figure S19–S20). Note that measurements taken from the G-1 are elevated relative to MBO due to their proximity to fire sources (Figure 2).

For each identified plume, MCE is calculated by determining the slope between CO and CO₂ using an unconstrained linear orthogonal distance regression and subsequently solving for $MCE = 1/(1+\Delta CO/\Delta CO_2)$. The ERs of various aerosol and gas-phase parameters with respect to ΣC for each plume are also calculated and expressed as $\Delta X/\Delta \Sigma C$, where X is a plume parameter of interest. The calculated MCE values range from 0.80 to 0.99 for the 18 plumes sampled at MBO and range from 0.86 to 0.96 for the 14 plumes sampled by the G-1. The ERs for most aerosol parameters with respect to ΣC were found to have

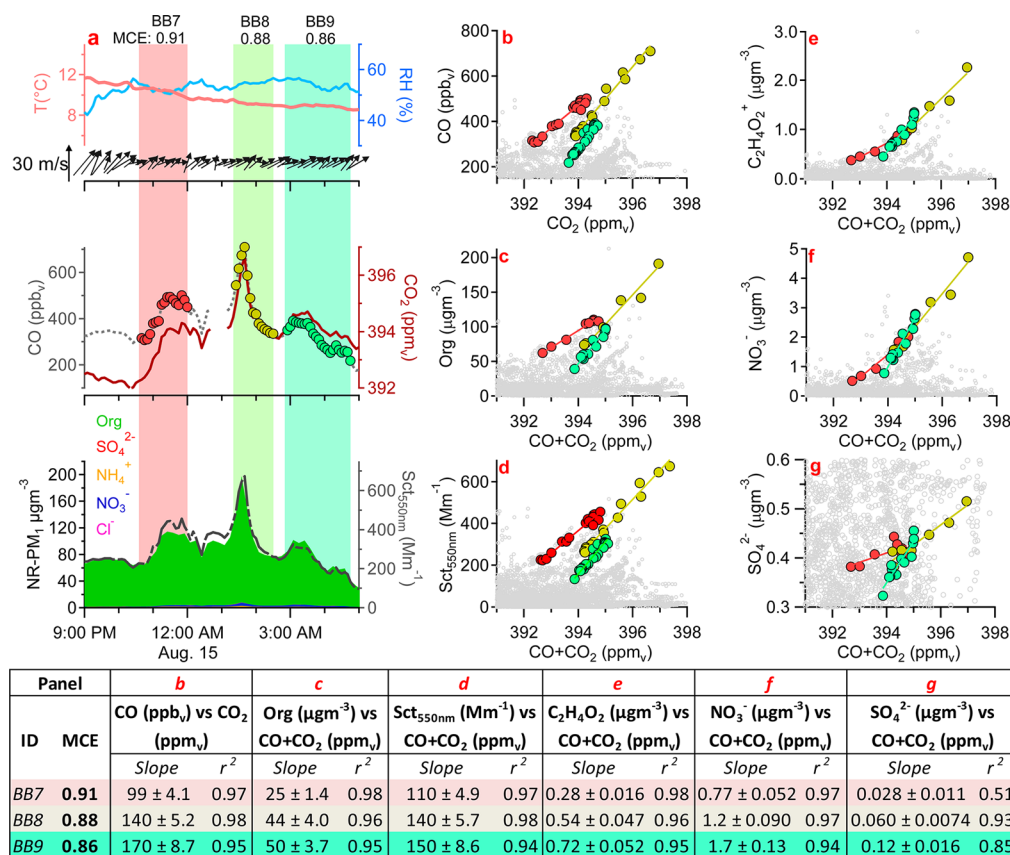


Figure 3. Detailed description of 3 consecutive plumes occurring during 21:00 PM 08/14/2013 to 5:00 AM 08/15/2013. (a) The time series of temperature, RH, wind direction and speed, CO and CO₂ mixing ratios, concentrations of individual NR-PM₁ species under standard conditions (shown as stacked), and total PM₁ scattering. The three plumes are highlighted with colored bars and corresponding MCE is displayed at the top of the graph. Scatter plots, with the same three plumes highlighted by the same colored markers and fit lines, as well as showing all data measured throughout campaign in gray markers are shown for (b) CO vs CO₂ and (c–g) organic PM₁, aerosol scattering, C₂H₄O₂⁺, nitrate and sulfate vs CO + CO₂. The table beneath the figures shows a summary of the slopes of the linear regressions depicted in Figure 2b–g and are defined here as the enhancement ratios.

a strong negative correlation with MCE and will be discussed further in sections 3.2 and 3.3. Most of the plumes appeared to come from fires occurring in southwest Oregon and northern California with a few arriving from northern Oregon (SI Figure S3–S17). Based on HYSPLIT air mass trajectories and MODIS fire locations, we estimate that the 32 BB plumes varied in their transport times between 1–48 h.

3.2. A Case Study of Three Consecutive Plumes Observed at MBO. Figure 3 shows an example of the identification of three BB plumes that impacted MBO on August 14th and 15th consecutively. These plumes all came from the Salmon River Fire Complex with a total transport time of approximately 12 h, suggesting that they had undergone a similar degree of atmospheric aging. Meteorological conditions were relatively stable during the designated plume time spans and wind was relatively constant (12 ± 2.9 m/s, southwesterly, Figure 3a). CO and CO₂ mixing ratios, aerosol scattering coefficient, and organic PM₁ mass concentrations were elevated during each plume period and had high intercorrelation (Figure 3). The MCE values of the three plumes decreased over time at 0.91, 0.88, and 0.86 (Figure 3b), indicating gradually decreased combustion efficiency.

BBOA is a dominant aerosol component in these plumes, accounting for >94% of the NR-PM₁ mass. The enhancement of BBOA relative to ΣC (i.e., $\Delta\text{Org}/\Delta\Sigma\text{C}$) increases as MCE decreases (Figure 3c), so do the enhancements of scattering

(550 nm, Figure 3d) and the AMS marker ions for anhydrous sugars (e.g., levoglucosan), C₂H₄O₂⁺ (Figure 3e) and C₃H₅O₂⁺.^{40,41} Inorganic nitrate (NO₃⁻, Figure 3f), although contributing a small percentage to the PM₁ mass, displays an enhancement that also correlates inversely with MCE. On the other hand, sulfate correlates less well with ΣC and does not appear significantly enhanced within the plume relative to nonplume periods (Figure 3g), indicating influences from sources other than wildfires. Since transport time and source are similar for all three plumes, the differences observed in ERs for BBOA, tracers, scattering and inorganic nitrate are likely due to changes in combustion processes.

3.3. Influence of MCE on Aerosol Emission Characteristics. The trends observed for the three consecutive plumes discussed above were also observed when examining all 32 plumes (Figure 4). A strong negative correlation between the ER of BBOA and MCE is observed and the values measured from both MBO and G-1 fall tightly along the same trend (Figure 4a). Since the estimated ages of the 32 BB plumes vary between ~1–48 h (6–48 h for MBO plumes and 1–6 h for G-1 plumes), this strong agreement suggests that net changes in BBOA concentrations were either slow or very similar plume to plume (i.e., independent to transport time).

One explanation is that BBOA is composed of primary organic aerosol (POA) directly emitted from the burning biomass and secondary organic aerosol (SOA) formed via

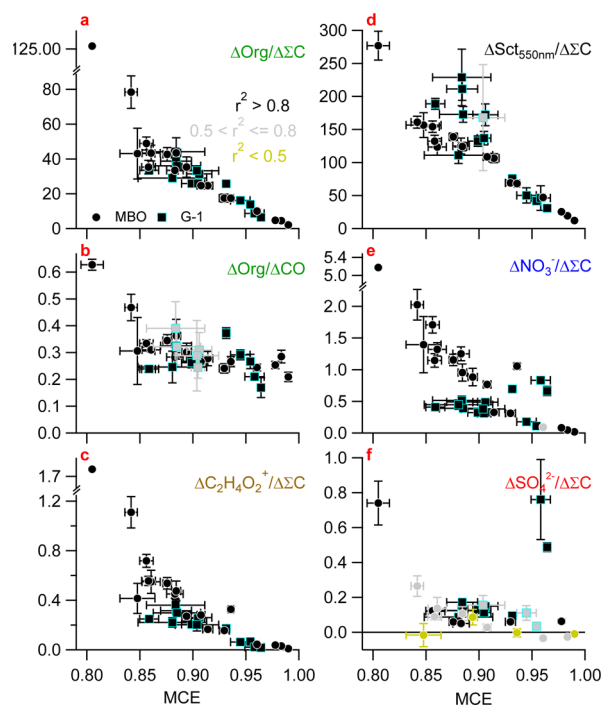


Figure 4. Enhancement ratios of (a–b) organic, (c) $C_2H_4O_2^+$, (d) aerosol light scattering, (e) nitrate and (f) sulfate relative to $CO+CO_2$ vs MCE except for (b) which is relative to CO vs MCE. ERs with respect to ΣC are in $\mu g\ m^{-3}/ppm_v$ for Org, NO_3 , and SO_4 , in org-equivalent $\mu g\ m^{-3}/ppm_v$ for $C_2H_4O_2^+$, and Mm^{-1}/ppm_v for scattering. ER of Org with respect to CO is in $\mu g\ m^{-3}/ppb_v$. Markers are either filled circles for MBO plumes or filled squares with a blue stroke for G-1 plumes and all are colored based on correlation coefficients between the given variable and $CO+CO_2$ or CO . Error bars for ER and MCE values represent the linear regressions errors of the calculated slopes. Note that axes are split for clarity for panels a, b, c, and e.

oxidative processing of organic gases. These two components are expected to exhibit opposite behaviors during transport, with POA evaporating with dilution due to the semivolatile nature of BBOA⁴² and SOA increasing with more atmospheric processing.⁴³ Indeed, thermal denuder data from MBO demonstrates the semivolatile nature of fresh BBOA.⁴³ Substantial net formation of SOA in BB emissions has been observed both in the laboratory^{44–46} and in the field,⁴⁷ though other field studies have not found significant enhancement of BBOA mass as BB emissions photochemically aged.^{36,48,49} This observed variability highlights the importance of fully characterizing BBOA properties and the complex processing that modifies these properties during atmospheric transport.

Our observations of negligible change in the apparent ERs of BBOA with transport time for a range of MCE values might be a combined, offsetting outcome of primary BBOA losses driven by dilution and subsequent evaporation of the semivolatile components,⁴² and SOA formation. On the other hand, the consistency among plumes measured in this work from the G-1 and MBO may reflect some similar processing among plumes or fast processing (e.g., < 1 h), which occurred near the source prior to sampling, then was followed by little net change in BBOA mass during subsequent atmospheric transport.

Additionally, Figure 4b shows the enhancement of organics with respect to ΔCO , which is often used to determine net formation of secondary components due to photochemical activity, particularly for transported plumes since CO is a stable

tracer and has low background concentrations. However, it is important to note that the relative amount of CO emitted is influenced by MCE as well. CO increases with decreasing MCE, thus $\Delta Org/\Delta CO$ is relatively flat for various MCEs and there is high consistency between MBO and G-1 plumes (Figure 4b) with the exception of plume 14 at MCE = 0.8 which has a significantly larger enhancement. Based on back-trajectory analysis, this plume appears to be of similar age to other plumes but originated from the Douglas Complex Fire, which was less frequently sampled at MBO during this study. Thus, the larger $\Delta Org/\Delta CO$ for this plume could be characteristic of smoldering fires, which are associated with higher VOC emissions and lower NO_x ,^{17,18} conditions which may lead to higher SOA forming potential over a wide range of aging time. Or larger $\Delta Org/\Delta CO$ could be due to differences in fuel type. Caution should be taken in this interpretation since a limited number of plumes were sampled in the lower MCE range (0.8–0.85).

A strong negative correlation of the ERs of the HR-AMS levoglucosan tracer ion ($C_2H_4O_2^{+41,50}$) and MCE is observed (Figure 4c), indicating that anhydrous sugars are emitted in larger quantities under less efficient combustion. This is consistent with the increased emissions of incomplete combustion products under more smoldering conditions. Furthermore, the overlap in ERs of this tracer ion in fresher and more aged plumes (Figure 4c) suggests few or similar losses of anhydrous sugars during atmospheric transport. Previous studies indicate that levoglucosan can undergo oxidation in the atmosphere,⁴⁵ particularly under cloudy conditions.⁵¹ We therefore examine relative humidity (RH) along each MBO plume trajectory derived via HYSPLIT back trajectory analysis and summarize the results of this analysis in SI Figure S18. According to RH values of air masses, all plumes experienced dry conditions (mean RH = 39% \pm 9.6%) along their trajectories before sampling at MBO, suggesting that aqueous oxidation was less likely to have affected levoglucosan enhancement ratios during this study.

The ER of aerosol light scattering determined from MBO clearly decreases as a function of MCE (Figure 4d), similar to the trend observed for the ER of organic aerosols (Figure 4a). However, those from G-1 measurements appear to deviate from the trend (Figure 4d), likely due to different size cutoff for particle sampling: MBO used a PM_{10} inlet, whereas G-1 used an isokinetic inlet (samples particles up to 5 μm in size), thus may have measured the scattering of coarse mode soil and dust particles.

The ERs of nitrate measured at MBO correlate inversely with MCE whereas those measured from G-1 have a more flat behavior (Figure 4e). Typically ERs of nitrogen-containing compounds measured near the source are indicative of fuel nitrogen content.¹⁵ Oxidized compounds such as NO_x dominate in flaming conditions whereas reduced compounds such as NH_3 dominate in smoldering conditions.¹⁶ In this case, however, the transport of these plumes complicates the interpretation. Due to photochemical processes, NO_x can be converted to more oxidized components such as peroxyacetyl nitrate (PAN) and nitrate.⁵² On the other hand, sulfate often displays poor correlations with ΣC and its ER values show little dependence on MCE (Figure 4f). These observations are consistent with previous findings that sulfur (S) content in biomass is highly variable and that the EF of S-containing species displays weak correlation with MCE in laboratory fires.^{19,53} The contributions of wildfires to sulfate appeared

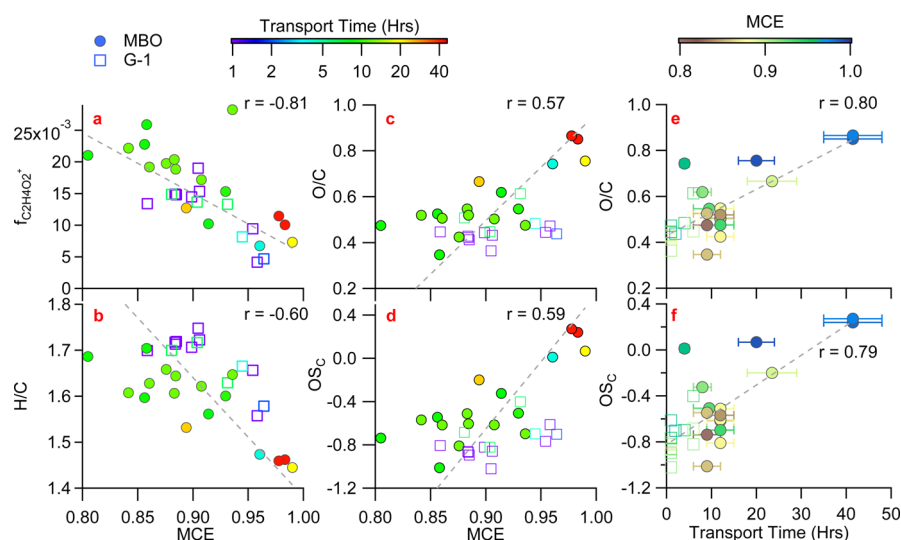


Figure 5. Parameters depicted here are derived from the ERMS calculated for each of the 32 plumes where solid circles are for MBO and open squares are for G-1. They include (a) the fractional contribution of $\text{C}_2\text{H}_4\text{O}_2^+$ to the total signal, (b) H/C, (c) O/C, and (d) OS_C vs MCE. All data points in a–d are colored by approximate transport time calculated based on HYSPLIT trajectory information. Panels e and f are the parameters O/C and OS_C , respectively, plotted vs transport time and points are colored by MCE. The Pearson's r correlation is reported in the top right panels for all parameters using least distance orthogonal fitting. The outlier in panel (a) at MCE = 0.94 and $f_{\text{C}_2\text{H}_4\text{O}_2^+} = 0.028$ was not included in Pearson's r correlation calculation. Note that almost no correlation was observed when fitting MCE vs Transport Time (see SI Figure S24).

negligible compared to background concentrations during this study and hence, sulfate appeared to be contributed by sources other than wildfires.

3.4. Influence of MCE on Chemical Properties of Organic Aerosol in Biomass Burning Plumes.

The chemical properties of BBOA observed for individual plumes are examined to determine whether a relationship between the organic aerosol chemistry and MCE existed or whether atmospheric aging had a larger influence. In this study, and ambient air in general, BB plumes often occurred as short-duration events over an elevated background of more aged aerosols. In order to isolate signals unique to the targeted plume from background contributions, we determined the ERs of the organic-equivalent mass concentrations of ions measured by the AMS by calculating their unconstrained linear regression slope with respect to ΣC . We defined an enhancement ratio mass spectrum (ERMS) by using the calculated slope of each ion as the signal contribution in the new ERMS and then normalized the total signal in the ERMS to 1. All 32 BB plumes were treated in the same way and a unique ERMS was derived for each plume to examine detailed chemical information on BBOA, such as elemental ratios (e.g., O/C and H/C), carbon oxidation state (OS_C), and fractional contributions of tracer ions (e.g., $f_{\text{C}_2\text{H}_4\text{O}_2^+}$). Note that for each plume, a vast majority of the ions show tight correlations with ΣC ($r^2 > 0.9$; e.g., see SI Figure S19–S20), which indicates the validity of using this approach to extract plume spectra. Ions with lower r^2 were retained, but they contribute <5% of the overall signal in the ERMS and consequently, their influence on calculated elemental ratios is considered negligible.

Figure 5 shows the chemical properties of BBOA derived from the ERMS of the 32 plumes as a function of MCE. The $f_{\text{C}_2\text{H}_4\text{O}_2^+}$ is used to assess the influence of BB on ambient aerosol.⁴⁰ Findings from lab studies regarding $f_{\text{C}_2\text{H}_4\text{O}_2^+}$ and combustion conditions have been variable with a residential wood burning experiment showing a positive correlation of $f_{\text{C}_2\text{H}_4\text{O}_2^+}$ with MCE⁵⁴ and a simulated open burning experiment

finding similar $f_{\text{C}_2\text{H}_4\text{O}_2^+}$ for both smoldering and flaming.⁴¹ In this study a decreasing trend with respect to MCE is observed for both the fresh (~ 1 –6 h of transport) and more aged (6–48 h of transport) plumes with very good agreement between the observations from MBO and G-1 (Figure 5a). These results reinforce the conclusion that the ERs of levoglucosan measured downwind appear to reflect those measured near the source, and that subsequent processing was either minimal or similar in all plumes. While a decrease of $f_{\text{C}_2\text{H}_4\text{O}_2^+}$ has been shown to correlate with aging of BBOA,^{40,55} our analysis suggests that MCE is an additional factor affecting $f_{\text{C}_2\text{H}_4\text{O}_2^+}$ for BBOA with less than 48 h of atmospheric aging. Hence caution should be exercised while using this tracer to probe the evolution of biomass burning aerosols in the atmosphere.

The H/C has a decreasing trend with respect to MCE (Figure 5b) whereas O/C increases with MCE (Figure 5c). In addition, OS_C ($= 2 \times \text{O/C} - \text{H/C}$), which is a more reliable metric for describing the average carbon oxidation state of organic aerosol,⁵⁶ also shows an increasing trend with MCE (Figure 5d). Other studies have measured the fractional contribution of CO_2^+ , a dominant ion fragment in highly oxidized organic aerosol,⁵⁷ to total BBOA signal (f_{44}) for various fuels under controlled conditions.^{54,58–60} One lab study showed that the relationship between f_{44} and MCE depended on fuel type, suggesting some fuel types led to more oxidized organic aerosol in flaming conditions.⁶⁰ Our results indicate relatively greater emissions of reduced organic compounds at lower MCE values, which is consistent with smoldering combustion (low MCE) emitting higher concentrations of both particulate and gaseous organic compounds and with BBOA often appearing semivolatile in nature. As MCE increases, the overall composition of BBOA becomes more oxidized and possibly less volatile. Furthermore, since the ER of BBOA is lower at high MCE, differential evaporation may cause preferential partitioning to the gas-phase of the semivolatile species, leaving a higher fraction of more oxidized components.⁶¹ However, the trends for O/C and OS_C as a function of

Table 1. Summary of Measured Aerosol Enhancement Parameter Statistics Divided into Smoldering (MCE < 0.9), Flaming (MCE > 0.9) and All Conditions for the 32 Plumes Measured at MBO and from G-1^a

		smoldering		flaming		all	
		mean	st dev	mean	st dev	mean	st dev
MCE		0.87	± 0.024	0.94	± 0.029	0.91	± 0.046
fC ₂ H ₄ O ₂		0.018	± 0.0039	0.012	± 0.0061	0.015	± 0.0058
fC ₄ H ₉		0.012	± 0.0029	0.010	± 0.0036	0.011	± 0.0033
H/C		1.7	± 0.056	1.6	± 0.098	1.6	± 0.084
O/C		0.47	± 0.078	0.57	± 0.16	0.52	± 0.13
OS _c		-0.71	± 0.20	-0.46	± 0.41	-0.59	± 0.34
OM/OC		1.8	± 0.10	1.9	± 0.20	1.8	± 0.17
ΔNH ₄ /ΔΣC	μgm ⁻³ /ppm _v	0.47	± 0.38	0.17	± 0.092	0.32	± 0.32
ΔNO ₃ /ΔΣC	μgm ⁻³ /ppm _v	1.2	± 1.2	0.40	± 0.32	0.81	± 0.94
ΔOrg/ΔΣC	μgm ⁻³ /ppm _v	46	± 25	17	± 10	31	± 24
ΔOrg/ΔCO	μgm ⁻³ /ppb _v	0.33	± 0.098	0.26	± 0.046	0.30	± 0.084
ΔOC/ΔΣC	gC/gC	0.049	± 0.028	0.017	± 0.010	0.033	± 0.026
ΔSct/ΔΣC *	Mm ⁻¹ /ppm _v	155	± 48	57	± 38	109	± 66

^aThe division between smoldering and flaming regimes is defined as MCE = 0.9, at which point an equal amount of smoldering and flaming combustion is present.^{16,64} Errors represent SD and number of independent data points, N = 16 and 16 for smoldering and flaming respectively.

* Scattering enhancement averages are for MBO data only.

MCE are not as clear for the fresher plumes sampled by G-1 closer to the fire sources and the G-1 plumes tend to be less oxidized overall compared to the more aged plumes sampled at MBO.

In order to investigate the effect that aging may have on the observed trends, all parameters in Figure 5a–d are colored by transport times estimated based on HYSPLIT trajectories and approximate overlap with MODIS fire hotspots and the relationship between O/C and OS_c and transport is shown explicitly in Figure 5e–f. Although relatively high uncertainty likely exists in the estimated transport time, the results suggest that transport time plays a larger role than MCE in determining the oxidation state of transported BBOA. In general, older plumes appear more oxidized for a given MCE value and the correlation between oxidation state and plume age appears somewhat higher (Figure 5e–f) than that between BBOA oxidation and MCE (Figure 5c–d). Nevertheless, MCE appears to be another factor affecting the average oxidation state of BBOA since a positive correlation is still visible. For instance, plumes at the highest MCE, despite having a large range in transport times, have significantly higher OS_c compared to lower MCE plumes (Figure 5d).

Smoldering combustion is dominated by the gasification of unburned fuel whereas flaming combustion is dominated by pyrolysis products which undergo in-flame processing.¹⁶ The results shown here demonstrate that the two burning regimes, along with atmospheric aging, may have affected the aerosol compositions measured downwind of the source, which tend to control particle properties and hence strongly influence their impact on regional air quality and climate change. This finding has important implications on our understanding of BBOA properties and how we model it to further understand the effects of BB emissions on a regional scale.

3.5. Implications for Models and Emissions Inventories. Our study has measured ERs and MCE values for a large number of wildfire plumes and highlights the dependence of aerosol emissions on MCE. Table 1 summarizes the average ERs for all 32 plumes as well as for smoldering- and flaming-dominated conditions separately where the division between smoldering and flaming is set to 0.9.^{16,64} Since the fuel complexes discussed in this study are representative of the

Pacific Northwest of the United States, our results are highly relevant for understanding typical temperate wildfires of evergreen vegetation. Emission ratios for similar biomes are shown for comparison in Figure 6, where a variety of sampling

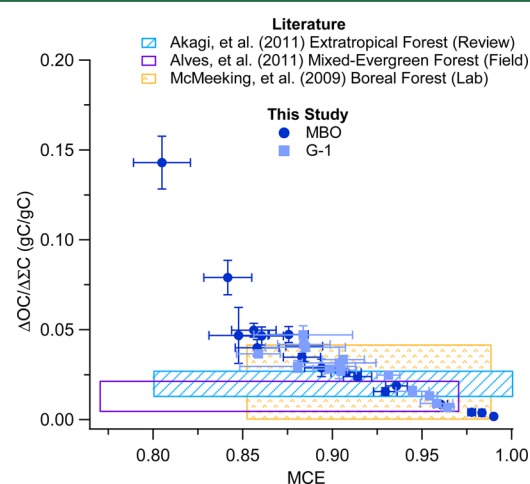


Figure 6. Emission ratios (ERs) of organic carbon determined in this study compared to ERs reported in literature using similar biomes. Error bars for ER and MCE values represent the linear regressions errors of the calculated slopes. Literature values are represented by boxes where top and bottom cover reported ER ranges and left and right sides cover reported MCE ranges. For ERs with no MCE reported the range is set to 0.8–1.0.

methods were used (see SI Table S3 for calculation method). The ERs of total organic carbon (OC) for our flaming plumes identified in this study (average $\pm 1\sigma = 0.017 \pm 0.010$ gC/gC; Table 1) compare well with literature “fire-average” results;^{4,19,62} however, the ERs of OC for the smoldering plumes (0.049 ± 0.028) are significantly higher than those reported by Alves et al.⁶² and Akagi et al.⁴ although our results fall within some lab-derived OC ER reported in McMeeking et al.¹⁹ save two plumes with MCE < 0.85. This illustrates that the emissions from a fire temporarily dominated by smoldering may not be well represented by fire-average emissions reported in literature.

Previous studies have demonstrated that MCE is a relevant parameter controlling emission factors for BB emissions near their source.^{18–21,63} Here we have found evidence that downwind ERs describing regional BBOA concentrations as well as chemical composition are influenced by MCE at the time of emission, implying that some of the relationships controlled by combustion processes at the source survived regional transport (<48 h). We have also demonstrated that the oxidation state of transported BBOA appears to be affected by both atmospheric aging and MCE. These results may serve in the future for modeling PM and trace gas emissions for this region. Furthermore, the method used in this study to identify plumes and extract enhancement ratio mass spectra as a function of MCE could be applied to data from other regions to explore broader applications and further understand the relationship between fuel types, combustion processes, and atmospheric aging on observed BBOA chemistry.

■ ASSOCIATED CONTENT

📄 Supporting Information

This material is available free of charge via the Internet at <http://pubs.acs.org/>. The Supporting Information is available free of charge on the ACS Publications website at DOI: 10.1021/acs.est.6b01617.

Detailed instrumental description and campaign overview with accompanying figures, back trajectory and forward trajectory analysis results, and tables summarizing main parameters described in main manuscript (PDF)

■ AUTHOR INFORMATION

Corresponding Author

*Phone: (530)752-5779; e-mail: dkwzhang@ucdavis.edu.

Notes

The authors declare no competing financial interest.

■ ACKNOWLEDGMENTS

This work was funded by US Department of Energy (DOE) Atmospheric Radiation Measurement (ARM) program and the Atmospheric System Research (ASR) program (Grants DE-SC0014620, DE-SC0007178, and DE-SC0014287) and used data from the ARM Climate Research Facility, a DOE Office of Science User Facility. MBO receives funding from the National Science Foundation (Grant NSF-1447832 to DJ). R.Y. was supported by NASA ACCDAM award NNX14AP45G. The Pacific Northwest National Laboratory is operated for DOE by Battelle Memorial Institute under contract DE-AC05-76RL01830. MKD thanks ASR grant F265 for support to LANL. We acknowledge the use of MODIS fire hotspot data and imagery from LANCE FIRMS, downloadable from <https://firms.modaps.eosdis.nasa.gov> and operated by the NASA/GSFC/Earth Science Data and Information System (ESDIS) with funding provided by NASA/HQ.

■ REFERENCES

- (1) de Gouw, J.; Jimenez, J. L. Organic Aerosols in the Earth's Atmosphere. *Environ. Sci. Technol.* **2009**, *43* (20), 7614–7618.
- (2) Bond, T. C.; Doherty, S. J.; Fahey, D. W.; Forster, P. M.; Bernsten, T.; DeAngelo, B. J.; Flanner, M. G.; Ghan, S.; Kärcher, B.; Koch, D.; Kinne, S.; Kondo, Y.; Quinn, P. K.; Sarofim, M. C.; Schultz, M. G.; Schulz, M.; Venkataraman, C.; Zhang, H.; Zhang, S.; Bellouin, N.; Guttikunda, S. K.; Hopke, P. K.; Jacobson, M. Z.; Kaiser, J. W.;

Klimont, Z.; Lohmann, U.; Schwarz, J. P.; Shindell, D.; Storelvmo, T.; Warren, S. G.; Zender, C. S. Bounding the role of black carbon in the climate system: A scientific assessment. *Journal of Geophysical Research: Atmospheres* **2013**, *118* (11), 5380–5552.

(3) Jaffe, D. A.; Wigder, N. L. Ozone production from wildfires: A critical review. *Atmos. Environ.* **2012**, *51* (0), 1–10.

(4) Akagi, S. K.; Yokelson, R. J.; Wiedinmyer, C.; Alvarado, M. J.; Reid, J. S.; Karl, T.; Crouse, J. D.; Wennberg, P. O. Emission factors for open and domestic biomass burning for use in atmospheric models. *Atmos. Chem. Phys.* **2011**, *11* (9), 4039–4072.

(5) Hobbs, P. V.; Reid, J. S.; Kotchenruther, R. A.; Ferek, R. J.; Weiss, R. Direct Radiative Forcing by Smoke from Biomass Burning. *Science* **1997**, *275* (5307), 1777–1778.

(6) Andreae, M. O.; Rosenfeld, D. Aerosol–cloud–precipitation interactions. Part 1. The nature and sources of cloud-active aerosols. *Earth-Sci. Rev.* **2008**, *89* (1–2), 13–41.

(7) Carrico, C. M.; Petters, M. D.; Kreidenweis, S. M.; Sullivan, A. P.; McMeeking, G. R.; Levin, E. J. T.; Engling, G.; Malm, W. C.; Collett, J. L. Water uptake and chemical composition of fresh aerosols generated in open burning of biomass. *Atmos. Chem. Phys.* **2010**, *10* (11), 5165–5178.

(8) IPCC, *IPCC—Climate Change 2013: The Physical Science Basis*, 2013.

(9) Andreae, M. O.; Rosenfeld, D.; Artaxo, P.; Costa, A. A.; Frank, G. P.; Longo, K. M.; Silva-Dias, M. A. F. Smoking Rain Clouds over the Amazon. *Science* **2004**, *303* (5662), 1337–1342.

(10) Duncan, B. N.; Martin, R. V.; Staudt, A. C.; Yevich, R.; Logan, J. A. Interannual and seasonal variability of biomass burning emissions constrained by satellite observations. *J. Geophys. Res.* **2003**, *108* (D2), ACH 1–1–ACH 1–22.

(11) Brewer, P.; Moore, T. Source Contributions to Visibility Impairment in the Southeastern and Western United States. *J. Air Waste Manage. Assoc.* **2009**, *59* (9), 1070–1081.

(12) Jaffe, D.; Hafner, W.; Chand, D.; Westerling, A.; Spracklen, D. Interannual Variations in PM_{2.5} due to Wildfires in the Western United States. *Environ. Sci. Technol.* **2008**, *42* (8), 2812–2818.

(13) Peltier, R. E.; Sullivan, A. P.; Weber, R. J.; Brock, C. A.; Wollny, A. G.; Holloway, J. S.; de Gouw, J. A.; Warneke, C. Fine aerosol bulk composition measured on WP-3D research aircraft in vicinity of the Northeastern United States: results from NEAQS. *Atmos. Chem. Phys.* **2007**, *7* (12), 3231–3247.

(14) Vicente, A.; Alves, C.; Calvo, A. I.; Fernandes, A. P.; Nunes, T.; Monteiro, C.; Almeida, S. M.; Pio, C. Emission factors and detailed chemical composition of smoke particles from the 2010 wildfire season. *Atmos. Environ.* **2013**, *71* (0), 295–303.

(15) Lobert, J. M.; Scharffe, D. H.; Hao, W. M.; Kuhlbusch, T. A.; Seuwan, R.; Warneck, P.; Crutzen, P. J., Experimental evaluation of biomass burning emissions: nitrogen and carbon containing compounds. In *Global Biomass Burning: Atmospheric, Climatic and Biospheric Implications*, Levine, J. S., Ed.; MIT Press: Cambridge, MA, 1991; pp 289–304.

(16) Yokelson, R. J.; Griffith, D. W. T.; Ward, D. E. Open-path Fourier transform infrared studies of large-scale laboratory biomass fires. *Journal of Geophysical Research: Atmospheres* **1996**, *101* (D15), 21067–21080.

(17) Yokelson, R. J.; Susott, R.; Ward, D. E.; Reardon, J.; Griffith, D. W. T. Emissions from smoldering combustion of biomass measured by open-path Fourier transform infrared spectroscopy. *Journal of Geophysical Research: Atmospheres* **1997**, *102* (D15), 18865–18877.

(18) Akagi, S. K.; Yokelson, R. J.; Burling, I. R.; Meinardi, S.; Simpson, I.; Blake, D. R.; McMeeking, G. R.; Sullivan, A.; Lee, T.; Kreidenweis, S.; Urbanski, S.; Reardon, J.; Griffith, D. W. T.; Johnson, T. J.; Weise, D. R. Measurements of reactive trace gases and variable O₃ formation rates in some South Carolina biomass burning plumes. *Atmos. Chem. Phys.* **2013**, *13* (3), 1141–1165.

(19) McMeeking, G. R.; Kreidenweis, S. M.; Baker, S.; Carrico, C. M.; Chow, J. C.; Collett, J. L.; Hao, W. M.; Holden, A. S.; Kirchstetter, T. W.; Malm, W. C.; Moosmüller, H.; Sullivan, A. P.; Wold, C. E.

Emissions of trace gases and aerosols during the open combustion of biomass in the laboratory. *J. Geophys. Res.* **2009**, *114* (D19), D19210.

(20) Yokelson, R. J.; Burling, I. R.; Urbanski, S. P.; Atlas, E. L.; Adachi, K.; Buseck, P. R.; Wiedinmyer, C.; Akagi, S. K.; Toohey, D. W.; Wold, C. E. Trace gas and particle emissions from open biomass burning in Mexico. *Atmos. Chem. Phys.* **2011**, *11* (14), 6787–6808.

(21) Burling, I. R.; Yokelson, R. J.; Akagi, S. K.; Urbanski, S. P.; Wold, C. E.; Griffith, D. W. T.; Johnson, T. J.; Reardon, J.; Weise, D. R. Airborne and ground-based measurements of the trace gases and particles emitted by prescribed fires in the United States. *Atmos. Chem. Phys.* **2011**, *11* (23), 12197–12216.

(22) Liu, S.; Aiken, A. C.; Arata, C.; Dubey, M. K.; Stockwell, C. E.; Yokelson, R. J.; Stone, E. A.; Jayathne, T.; Robinson, A. L.; DeMott, P. J.; Kreidenweis, S. M. Aerosol single scattering albedo dependence on biomass combustion efficiency: Laboratory and field studies. *Geophys. Res. Lett.* **2014**, *41* (2), 2013GL058392.

(23) Janhäll, S.; Andreae, M. O.; Pöschl, U. Biomass burning aerosol emissions from vegetation fires: particle number and mass emission factors and size distributions. *Atmos. Chem. Phys.* **2010**, *10* (3), 1427–1439.

(24) McMeeking, G. R.; Fortner, E.; Onasch, T. B.; Taylor, J. W.; Flynn, M.; Coe, H.; Kreidenweis, S. M. Impacts of nonrefractory material on light absorption by aerosols emitted from biomass burning. *Journal of Geophysical Research: Atmospheres* **2014**, *119* (21), 12,272–12,286.

(25) Canagaratna, M.; Jayne, J.; Jimenez, J. L.; Allan, J. A.; Alfarra, R.; Zhang, Q.; Onasch, T.; Drewnick, F.; Coe, H.; Middlebrook, A.; Delia, A.; Williams, L.; Trimborn, A.; Northway, M.; DeCarlo, P.; Kolb, C.; Davidovits, P.; Worsnop, D. Chemical and Microphysical Characterization of Ambient Aerosols with the Aerodyne Aerosol Mass Spectrometer. *Mass Spectrom. Rev.* **2007**, *26*, 185–222.

(26) DeCarlo, P. F.; Kimmel, J. R.; Trimborn, A.; Northway, M. J.; Jayne, J. T.; Aiken, A. C.; Gonin, M.; Fuhrer, K.; Horvath, T.; Docherty, K. S.; Worsnop, D. R.; Jimenez, J. L. Field-Deployable, High-Resolution, Time-of-Flight Aerosol Mass Spectrometer. *Anal. Chem.* **2006**, *78* (24), 8281–8289.

(27) Aiken, A. C.; DeCarlo, P. F.; Kroll, J. H.; Worsnop, D. R.; Huffman, J. A.; Docherty, K.; Ulbrich, I. M.; Mohr, C.; Kimmel, J. R.; Sueper, D.; Sun, Y.; Zhang, Q.; Trimborn, A.; Northway, M.; Ziemann, P. J.; Canagaratna, M. R.; Onasch, T. B.; Alfarra, M. R.; Prevot, A. S. H.; Dommen, J.; Duplissy, J.; Metzger, A.; Baltensperger, U.; Jimenez, J. L. O/C and OM/OC Ratios of Primary, Secondary, and Ambient Organic Aerosols with a High Resolution Time-of-Flight Aerosol Mass Spectrometer. *Environ. Sci. Technol.* **2008**, *42* (12), 4478–4485.

(28) Canagaratna, M. R.; Jimenez, J. L.; Kroll, J. H.; Chen, Q.; Kessler, S. H.; Massoli, P.; Hildebrandt Ruiz, L.; Fortner, E.; Williams, L. R.; Wilson, K. R.; Surratt, J. D.; Donahue, N. M.; Jayne, J. T.; Worsnop, D. R. Elemental ratio measurements of organic compounds using aerosol mass spectrometry: characterization, improved calibration, and implications. *Atmos. Chem. Phys.* **2015**, *15* (1), 253–272.

(29) Onasch, T. B.; Trimborn, A.; Fortner, E. C.; Jayne, J. T.; Kok, G. L.; Williams, L. R.; Davidovits, P.; Worsnop, D. R. Soot Particle Aerosol Mass Spectrometer: Development, Validation, and Initial Application. *Aerosol Sci. Technol.* **2012**, *46* (7), 804–817.

(30) Brechtel, F. *Description and assessment of a new aerosol inlet for the DOE G-1 research aircraft, Final technical report of work performed by BMI under contract #0000058843*; Brookhaven National Laboratory: 2003.

(31) Bahreini, R.; Dunlea, E. J.; Matthew, B. M.; Simons, C.; Docherty, K. S.; DeCarlo, P. F.; Jimenez, J. L.; Brock, C. A.; Middlebrook, A. M. Design and Operation of a Pressure-Controlled Inlet for Airborne Sampling with an Aerodynamic Aerosol Lens. *Aerosol Sci. Technol.* **2008**, *42* (6), 465–471.

(32) Lack, D. A.; Corbett, J. J.; Onasch, T.; Lerner, B.; Massoli, P.; Quinn, P. K.; Bates, T. S.; Covert, D. S.; Coffman, D.; Sierau, B.; Herndon, S.; Allan, J.; Baynard, T.; Lovejoy, E.; Ravishankara, A. R.; Williams, E. Particulate emissions from commercial shipping: Chemical, physical, and optical properties. *J. Geophys. Res.* **2009**, *114* (D7), D00F04.

(33) Kimmel, J. R.; Farmer, D. K.; Cubison, M. J.; Sueper, D.; Tanner, C.; Nemitz, E.; Worsnop, D. R.; Gonin, M.; Jimenez, J. L. Real-time aerosol mass spectrometry with millisecond resolution. *Int. J. Mass Spectrom.* **2011**, *303* (1), 15–26.

(34) Collier, S.; Zhang, Q. Gas-Phase CO₂ Subtraction for Improved Measurements of the Organic Aerosol Mass Concentration and Oxidation Degree by an Aerosol Mass Spectrometer. *Environ. Sci. Technol.* **2013**, *47* (24), 14324–14331.

(35) Draxler, R. R.; Hess, G. An overview of the HYSPLIT₄ modelling system for trajectories. *Australian Meteorological Magazine* **1998**, *47* (4), 295–308.

(36) Jolleys, M. D.; Coe, H.; McFiggans, G.; Capes, G.; Allan, J. D.; Crosier, J.; Williams, P. I.; Allen, G.; Bower, K. N.; Jimenez, J. L.; Russell, L. M.; Grutter, M.; Baumgardner, D. Characterizing the Aging of Biomass Burning Organic Aerosol by Use of Mixing Ratios: A Meta-analysis of Four Regions. *Environ. Sci. Technol.* **2012**, *46* (24), 13093–13102.

(37) Briggs, N. L.; Jaffe, D. A.; Gao, H.; Hee, J.; Baylon, P.; Zhang, Q.; Zhou, S.; Collier, S.; Sampson, P.; Cary, R. A. Particulate matter, ozone, and nitrogen species in aged wildfire plumes observed at the Mount Bachelor Observatory, a high elevation site in the Pacific Northwest. *Aerosol Air Qual. Res.* **2016**, DOI: 10.4209/aaqr.2016.03.0120.

(38) Yokelson, R. J.; Andreae, M. O.; Akagi, S. K. Pitfalls with the use of enhancement ratios or normalized excess mixing ratios measured in plumes to characterize pollution sources and aging. *Atmos. Meas. Tech.* **2013**, *6* (8), 2155–2158.

(39) Wigder, N. L.; Jaffe, D. A.; Saketa, F. A. Ozone and particulate matter enhancements from regional wildfires observed at Mount Bachelor during 2004–2011. *Atmos. Environ.* **2013**, *75* (0), 24–31.

(40) Cubison, M. J.; Ortega, A. M.; Hayes, P. L.; Farmer, D. K.; Day, D.; Lechner, M. J.; Brune, W. H.; Apel, E.; Diskin, G. S.; Fisher, J. A.; Fuelberg, H. E.; Hecobian, A.; Knapp, D. J.; Mikoviny, T.; Riemer, D.; Sachse, G. W.; Sessions, W.; Weber, R. J.; Weinheimer, A. J.; Wisthaler, A.; Jimenez, J. L. Effects of aging on organic aerosol from open biomass burning smoke in aircraft and laboratory studies. *Atmos. Chem. Phys.* **2011**, *11* (23), 12049–12064.

(41) Lee, T.; Sullivan, A. P.; Mack, L.; Jimenez, J. L.; Kreidenweis, S. M.; Onasch, T. B.; Worsnop, D. R.; Malm, W.; Wold, C. E.; Hao, W. M.; Collett, J. L. Chemical Smoke Marker Emissions During Flaming and Smoldering Phases of Laboratory Open Burning of Wildland Fuels. *Aerosol Sci. Technol.* **2010**, *44* (9), i–v.

(42) May, A. A.; Levin, E. J. T.; Hennigan, C. J.; Riiipinen, I.; Lee, T.; Collett, J. L.; Jimenez, J. L.; Kreidenweis, S. M.; Robinson, A. L. Gas-particle partitioning of primary organic aerosol emissions: 3. Biomass burning. *Journal of Geophysical Research: Atmospheres* **2013**, *118* (19), 2013JD020286.

(43) Zhou, S.; Collier, S. C.; Jaffe, D. A.; Briggs, N. L.; Hee, J.; Sedlacek, A. J., III; Kleinman, L.; Zhang, Q. Regional Influence of Wildfires on Aerosol Chemistry in the Western US and Insights into Atmospheric Aging of Biomass Burning Organic Aerosol. *Atmos. Chem. Phys.* **2016**, In Preparation.

(44) Ortega, A. M.; Day, D. A.; Cubison, M. J.; Brune, W. H.; Bon, D.; de Gouw, J. A.; Jimenez, J. L. Secondary organic aerosol formation and primary organic aerosol oxidation from biomass-burning smoke in a flow reactor during FLAME-3. *Atmos. Chem. Phys.* **2013**, *13* (22), 11551–11571.

(45) Hennigan, C. J.; Miracolo, M. A.; Engelhart, G. J.; May, A. A.; Presto, A. A.; Lee, T.; Sullivan, A. P.; McMeeking, G. R.; Coe, H.; Wold, C. E.; Hao, W. M.; Gilman, J. B.; Kuster, W. C.; de Gouw, J.; Schichtel, B. A.; Collett, J. L.; Kreidenweis, S. M.; Robinson, A. L. Chemical and physical transformations of organic aerosol from the photo-oxidation of open biomass burning emissions in an environmental chamber. *Atmos. Chem. Phys.* **2011**, *11* (15), 7669–7686.

(46) Grieshop, A. P.; Donahue, N. M.; Robinson, A. L. Laboratory investigation of photochemical oxidation of organic aerosol from wood fires 2: analysis of aerosol mass spectrometer data. *Atmos. Chem. Phys.* **2009**, *9* (6), 2227–2240.

- (47) Vakkari, V.; Kerminen, V.-M.; Beukes, J. P.; Tiitta, P.; van Zyl, P. G.; Josipovic, M.; Venter, A. D.; Jaars, K.; Worsnop, D. R.; Kulmala, M.; Laakso, L. Rapid changes in biomass burning aerosols by atmospheric oxidation. *Geophys. Res. Lett.* **2014**, *41* (7), 2644–2651.
- (48) Capes, G.; Johnson, B.; McFiggans, G.; Williams, P. I.; Haywood, J.; Coe, H. Aging of biomass burning aerosols over West Africa: Aircraft measurements of chemical composition, microphysical properties, and emission ratios. *J. Geophys. Res.* **2008**, *113* (D23), D00C15.
- (49) Jolleys, M. D.; Coe, H.; McFiggans, G.; Taylor, J. W.; O'Shea, S. J.; Le Breton, M.; Bauguitte, S. J. B.; Müller, S.; Di Carlo, P.; Aruffo, E.; Palmer, P. I.; Lee, J. D.; Percival, C. J.; Gallagher, M. W. Properties and evolution of biomass burning organic aerosol from Canadian boreal forest fires. *Atmos. Chem. Phys.* **2015**, *15* (6), 3077–3095.
- (50) Schneider, J.; Weimer, S.; Drewnick, F.; Borrmann, S.; Helas, G.; Gwaze, P.; Schmid, O.; Andreae, M. O.; Kirchner, U. Mass spectrometric analysis and aerodynamic properties of various types of combustion-related aerosol particles. *Int. J. Mass Spectrom.* **2006**, *258* (1–3), 37–49.
- (51) Arangio, A. M.; Slade, J. H.; Berkemeier, T.; Pöschl, U.; Knopf, D. A.; Shiraiwa, M. Multiphase Chemical Kinetics of OH Radical Uptake by Molecular Organic Markers of Biomass Burning Aerosols: Humidity and Temperature Dependence, Surface Reaction, and Bulk Diffusion. *J. Phys. Chem. A* **2015**, *119* (19), 4533–4544.
- (52) Akagi, S. K.; Craven, J. S.; Taylor, J. W.; McMeeking, G. R.; Yokelson, R. J.; Burling, I. R.; Urbanski, S. P.; Wold, C. E.; Seinfeld, J. H.; Coe, H.; Alvarado, M. J.; Weise, D. R. Evolution of trace gases and particles emitted by a chaparral fire in California. *Atmos. Chem. Phys.* **2012**, *12* (3), 1397–1421.
- (53) May, A. A.; McMeeking, G. R.; Lee, T.; Taylor, J. W.; Craven, J. S.; Burling, I.; Sullivan, A. P.; Akagi, S.; Collett, J. L.; Flynn, M.; Coe, H.; Urbanski, S. P.; Seinfeld, J. H.; Yokelson, R. J.; Kreidenweis, S. M. Aerosol emissions from prescribed fires in the United States: A synthesis of laboratory and aircraft measurements. *Journal of Geophysical Research: Atmospheres* **2014**, *119*, 2014JD021848.
- (54) Weimer, S.; Alfarra, M.; Schreiber, D.; Mohr, M.; Prévôt, A.; Baltensperger, U., Organic aerosol mass spectral signatures from wood-burning emissions: Influence of burning conditions and wood type. *J. Geophys. Res.* **2008**, *113*, (D10).[10.1029/2007JD009309](https://doi.org/10.1029/2007JD009309)
- (55) Hecobian, A.; Liu, Z.; Hennigan, C. J.; Huey, L. G.; Jimenez, J. L.; Cubison, M. J.; Vay, S.; Diskin, G. S.; Sachse, G. W.; Wisthaler, A.; Mikoviny, T.; Weinheimer, A. J.; Liao, J.; Knapp, D. J.; Wennberg, P. O.; Kürten, A.; Crouse, J. D.; Clair, J. S.; Wang, Y.; Weber, R. J. Comparison of chemical characteristics of 495 biomass burning plumes intercepted by the NASA DC-8 aircraft during the ARCTAS/CARB-2008 field campaign. *Atmos. Chem. Phys.* **2011**, *11* (24), 13325–13337.
- (56) Kroll, J. H.; Donahue, N. M.; Jimenez, J. L.; Kessler, S. H.; Canagaratna, M. R.; Wilson, K. R.; Altieri, K. E.; Mazzoleni, L. R.; Wozniak, A. S.; Bluhm, H.; Mysak, E. R.; Smith, J. D.; Kolb, C. E.; Worsnop, D. R. Carbon oxidation state as a metric for describing the chemistry of atmospheric organic aerosol. *Nat. Chem.* **2011**, *3* (2), 133–139.
- (57) Zhang, Q.; Alfarra, M. R.; Worsnop, D. R.; Allan, J. D.; Coe, H.; Canagaratna, M. R.; Jimenez, J. L. Deconvolution and Quantification of Hydrocarbon-like and Oxygenated Organic Aerosols Based on Aerosol Mass Spectrometry. *Environ. Sci. Technol.* **2005**, *39* (13), 4938–4952.
- (58) Heringa, M. F.; DeCarlo, P. F.; Chirico, R.; Lauber, A.; Doberer, A.; Good, J.; Nussbaumer, T.; Keller, A.; Burtscher, H.; Richard, A.; Miljevic, B.; Prevot, A. S. H.; Baltensperger, U. Time-Resolved Characterization of Primary Emissions from Residential Wood Combustion Appliances. *Environ. Sci. Technol.* **2012**, *46* (20), 11418–11425.
- (59) Heringa, M. F.; DeCarlo, P. F.; Chirico, R.; Tritscher, T.; Dommen, J.; Weingartner, E.; Richter, R.; Wehrle, G.; Prévôt, A. S. H.; Baltensperger, U. Investigations of primary and secondary particulate matter of different wood combustion appliances with a high-resolution time-of-flight aerosol mass spectrometer. *Atmos. Chem. Phys.* **2011**, *11* (12), 5945–5957.
- (60) Jolleys, M. D.; Coe, H.; McFiggans, G.; McMeeking, G. R.; Lee, T.; Kreidenweis, S. M.; Collett, J. L.; Sullivan, A. P. Organic aerosol emission ratios from the laboratory combustion of biomass fuels. *Journal of Geophysical Research: Atmospheres* **2014**, *119* (22), 12,850–12,871.
- (61) May, A. A.; Lee, T.; McMeeking, G. R.; Akagi, S.; Sullivan, A. P.; Urbanski, S.; Yokelson, R. J.; Kreidenweis, S. M. Observations and analysis of organic aerosol evolution in some prescribed fire smoke plumes. *Atmos. Chem. Phys. Discuss.* **2015**, *15* (2), 1953–1988.
- (62) Alves, C. A.; Vicente, A.; Monteiro, C.; Gonçalves, C.; Evtyugina, M.; Pio, C. Emission of trace gases and organic components in smoke particles from a wildfire in a mixed-evergreen forest in Portugal. *Sci. Total Environ.* **2011**, *409* (8), 1466–1475.
- (63) Christian, T. J.; Kleiss, B.; Yokelson, R. J.; Holzinger, R.; Crutzen, P. J.; Hao, W. M.; Saharjo, B. H.; Ward, D. E. Comprehensive laboratory measurements of biomass-burning emissions: 1. Emissions from Indonesian, African, and other fuels. *J. Geophys. Res.* **2003**, *108* (D23), 4719.
- (64) Ward, D. E.; Hardy, C. C. Smoke emissions from wildland fires. *Environ. Int.* **1991**, *17* (2–3), 117–134.